Nuclear Physics B (Proc. Suppl.) 37B (1994) 23–31
North-Holland

NUCLEAR PHYSICS B
PROCEEDINGS
SUPPLEMENTS

A Precise Measurement of the Left-Right Asymmetry of Z Boson Production at the SLAC Linear Collider

The SLD Collaboration
represented by R. C. King [a*]

[a]Stanford Linear Accelerator Center
P.O. Box 4349, MS 78
Stanford CA 94309, U.S.A.

During the 1993 run of the SLC/SLD, the SLD recorded 49,392 Z events produced by the collision of longitudinally polarized electrons on unpolarized positrons at a center-of-mass energy of 91.26 GeV. A Compton polarimeter measured to luminosity-weighted average polarization to be (63.0±1.1)%. A_{LR} was measured to be 0.1628±0.0071(stat.)±0.0028(syst.) which determines the effective weak mixing angle to be $\sin^2\theta_W^{\rm eff} = 0.2292 \pm 0.0009(\text{stat.}) \pm 0.0004(\text{syst.})$.

1. Introduction

In 1992, the SLD Collaboration performed the first measurement of the left-right cross section asymmetry (A_{LR}) in the production of Z bosons by e^+e^- collisions [1]. In these proceedings, we present a substantially more precise result that is based upon data recorded during the 1993 run of the SLAC Linear Collider (SLC) [2].

2. Properties of A_{LR}

For fermion/anti-fermion collisons at the Z pole energy one can rigorously define the fermion asymmetry, A_f. To leading order, the Standard Model predicts that this quantity depends upon the vector (v_f) and axial-vector (a_f) couplings of the Z boson to the fermion current

$$A_f \equiv (\sigma_L - \sigma_R)/(\sigma_L + \sigma_R) = \frac{2v_f a_f}{v_f^2 + a_f^2} \qquad (1)$$

where σ_L is the total production cross section when the fermion is left-handed, which is to say, its spin is anti-parallel to its momentum, and σ_R is the cross section when the fermion is right-handed.

The fermion asymmetry is insensitive to QCD and QED corrections (excepting initial state radiation), and to the final state of the Z decay. However, higher order electroweak processes do have a large effect on A_f. The main contributions come from the oblique and vertex corrections, the effects of which are absorbed into new coupling constants, $v_f^{\rm eff}$ and $a_f^{\rm eff}$.

For the particular case of an electron-positron collider, the fermion asymmetry in question is the electron asymmetry, A_e, which is also referred to as A_{LR} [3]. This quantity is related to the Weinberg angle though the following expression

$$A_{LR}^0 = A_{LR}(M_Z) = \frac{2\left[1 - 4\sin^2\theta_W^{\rm eff}\right]}{1 + \left[1 - 4\sin^2\theta_W^{\rm eff}\right]^2} \qquad (2)$$

where the effective electroweak mixing parameter is defined [4] as $\sin^2\theta_W^{\rm eff} \equiv (1 - v_f^{\rm eff}/a_f^{\rm eff})/4$. Note that A_{LR} is a sensitive function of $\sin^2\theta_W^{\rm eff}$ and therefore sensitive to electroweak radiative corrections, including those which involve the top quark, the Higgs boson, and new phenomena.

In a real experiment, the electron polarization is always less than 100%. Also, because of initial state radiation, no real experiment can occur exactly on the Z pole, and therefore the measured A_{LR} will be a function of center-of-mass energy, with a value different from A_{LR}^0. The measured asymmetry, A_m, is related to the energy-

*Work supported in part by the Department of Energy, contract DE-AC03-76SF00515.

1994 – Elsevier Science B.V.
SSDI 0920-5632(94)00608-3

dependent A_{LR} through the following equation:

$$A_m \equiv \frac{(N_L - N_R)}{(N_L + N_R)} = \langle \mathcal{P}_e \rangle A_{LR} \qquad (3)$$

where N_L and N_R are the observed number of left-handed and right-handed Z productions, and $\mathcal{P}_e$ is the longitudinal polarization at the SLC interaction point (IP). Throughout this document, we will use the "$\langle\rangle$" symbol to denote the luminosity-weighted average of a quantity over the time of the sample. Equation 3 assumes that all left-right asymmetries in polarization, luminosity, and other quantites are zero. Corrections to this assumption are discussed in section 7. However, to first order, the error on A_{LR} is given by

$$\delta A_{LR} = \sqrt{\frac{1}{\langle \mathcal{P}_e \rangle^2 N} + A_{LR}^2 \left(\frac{\delta \langle \mathcal{P}_e \rangle}{\langle \mathcal{P}_e \rangle} \right)^2}. \qquad (4)$$

It is clear from this relation that the statistical error on A_{LR} is a strong function of the electron polarization, and that the uncertainty in the polarization measurement is the dominant systematic error in the experiment.

Measuring A_{LR} requires three main components: a machine capable of accelerating polarized electrons, a method of monitoring the beam polarization, and a method of detecting Zs. At SLAC, these requirements are met by the polarized SLC, the Compton polarimter, and the SLD detector.

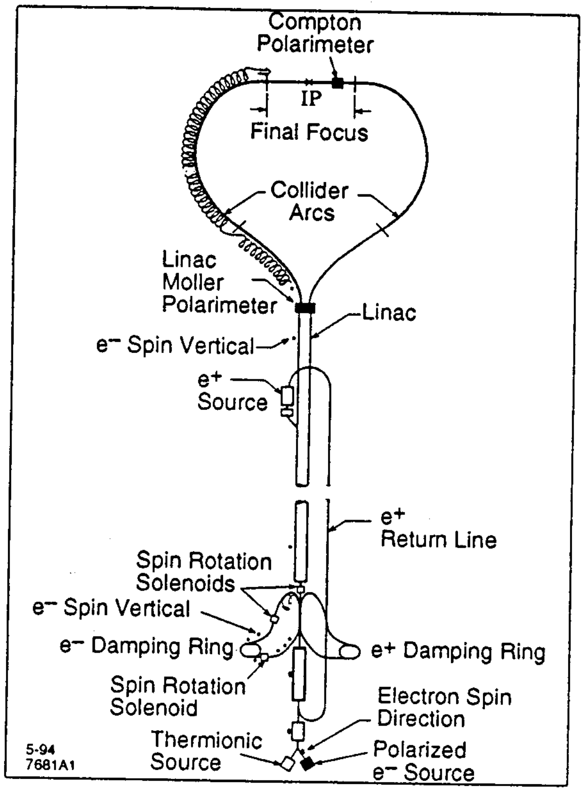

Figure 1. The SLAC Linear Collider

3. The Polarized SLC

The operation of the SLC with a polarized electron beam has been described previously [5]. Referring to figure 1, electrons are extracted longitudinally from the source, after which they are accelerated to 1.19 GeV and injected into the damping ring. The linac-to-ring (LTR) dipole section rotates the spin into the horizontal direction, and the LTR solenoid rotates the spin into the vertical direction for storage in the damping ring, where horizontal spin components will be randomized. Electrons are extracted from the damping ring after cooling for 8.8 ms, and are accelerated to their maximum energy ($\simeq$46.1 GeV) at the end of the linac. At this point the beam polarization is $\mathcal{P}_e^{linac}$. In the SLC arc, the electrons lose energy though synchrotron emission, and lose polarization through *spin diffusion* (defined in section 3.2). At the SLC interaction point the electron polarization is $\mathcal{P}_e$. The electrons continue past the IP to the Compton interaction point, where the polarization is measured to be $\mathcal{P}_e^C$.

In 1993, the maximum luminosity of the collider was increased to 5×10^{29} cm^2/sec by the use of flat (elliptical) beams which had transverse aspect ratios of 3/1 [6]. The luminosity-weighted mean e^+e^- center-of-mass energy (E_{cm}) is measured with precision energy spectrometers [7] to be 91.26$\pm$0.02 GeV.

Table 1 summarizes the performance of the SLC in 1993 and gives projections for the 1994 run.

Parameter	1993	1994 (projected)
N^+	3×10^{10}	$(3.5 - 4.0) \times 10^{10}$
N^-	3×10^{10}	$(3.5 - 4.0) \times 10^{10}$
f_rep	120 Hz	120 Hz
σ_x	0.8 μm	$(0.4 - 0.5)$ μm
σ_y	2.6 μm	2.4 μm
Z/hr (peak)	50	100
Energy	91.26 GeV	91.26 GeV
Polarization	63%	80%
Uptime	70%	70%
Run Time	6 months	6 months
Integrated Zs	50K	100K - 150K

Table 1
SLC Operational Parameters

3.1. The Polarized Electron Source

In addition to enhanced luminosity, the 1993 run of the SLC also featured enhanced beam polarization. The beam polarization at the SLC source was increased to over 65% by the use of a strained-lattice gallium-arsenide (GaAs) photocathode [8] illuminated by a pulsed Ti-Sapphire laser operating at 865 nm [9]. Strained-lattice cathodes are manufactured by growing a 0.1-0.3 micron layer of pure GaAs on a 2.5 micron gallium-arsenide-phosphide ($GaAs_{.76}P_{.24}$) substrate. $GaAs_{.76}P_{.24}$ has a smaller lattice spacing constant that GaAs, and the resulting strain caused by this mismatch is just enough to break the $P_{3/2}$ energy level degeneracy in the GaAs valence band, which in turn allows the excitation of a single electron polarization state by an incident circularly polarized photon bunch.

The circular polarization of the incident photons is controlled by the voltage setting on an electro-optic element known as a Pockels cell. As in 1992, the voltage state of the source Pockels cell (and hence, the helicity of each electron pulse) was chosen randomly on a pulse-by-pulse basis. The helicity information is transmitted and incorporated into the SLD event data stream. The synchronization of this transmission has been rigorously tested, and three independent systems are used to ensure the integrity of the transmission.

3.2. Spin Transport

The flat-beam mode of operation precludes the use of the two solenoidal spin rotator magnets (located downstream of the electron damping ring) that were used previously to orient the electron spin direction prior to acceleration in the linac. Therefore, the vertical spin orientation of the beam in the north damping ring is maintained during acceleration and launch into the SLC North Arc. A pair of large amplitude betatron oscillations in the arc is used to adjust the spin direction [10] to achieve longitudinal polarization at the SLC IP.

The spin precession angle, θ_s, for electrons in a dipole field is given by

$$\theta_s = \gamma\left(\frac{g-2}{2}\right)\theta_b \tag{5}$$

where θ_b is the bend angle of the electron momentum induced by the field. The product of γ ($\simeq E/m$ for large E), and $\frac{g-2}{2}$, the anomalous magetic moment of the electron. is known as the *spin tune* and is on the order of 100 at SLC energies. Because θ_s is a strong function of E, electrons within the bunch with slightly different energies will undergo different spin precessions. Loss of polarization resulting from this effect is called *spin diffusion.*

The longitudinal polarization of the electron beam at the IP is typically 95-96% of the polarization in the linac, as a result of imperfect spin orientation and energy-spread-induced spin diffusion in the SLC arc. This result follows from measurements of the arc spin rotation matrix performed with a beam of very small energy spread ($\leq$ 0.1%) using the spin rotation solenoids and the Compton polarimeter. These measurements determine the electron polarization in the linac to be (65.7±0.9)%. On several occasions, the beam polarization at end of the linac ($\mathcal{P}_e^{linac}$) was directly measured with a diagnostic Møller polarimeter and was found to be (66±3)% [11].

4. Polarimetry

The longitudinal electron beam polarization is measured by a Compton scattering polarimeter [12], depicted in figure 2. After it passes through

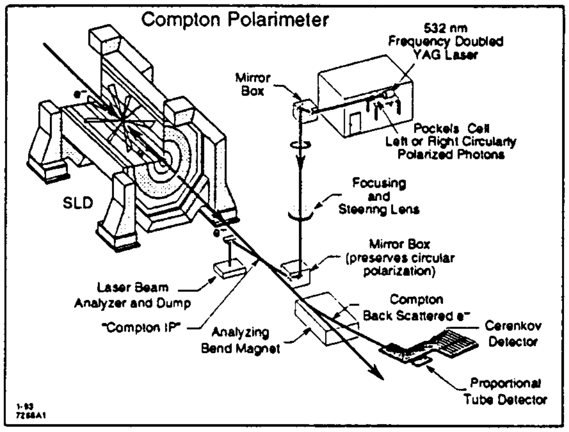

Figure 2. The Compton Polarimeter

the IP, the electron beam travels 33 m downstream and, before it encounters any dipole fields (and hence, before any spin precession occurs), collides with a circularly polarized photon target. The photons are produced by a frequency-doubled Nd:YAG laser of wavelength 532 nm. The scattered and unscattered components of the electron beam remain unseparated until they pass through a pair of analyzing dipole magnets. The scattered electrons are dispersed horizontally and exit the vacuum system through a thin window. They then shower in a 1.4 λ lead pre-radiator, which enhances the signal-to-noise ratio in the detector.

Polarimeter data are acquired continually during the operation of the SLC. The measured beam polarization is typically 61-64%. The absolute statistical precision attained in a 3 minute interval is typically $\delta\mathcal{P}_e = 1.0\%$.

4.1. The Compton Cherenkov Detector

The detector used for the polarimeter analysis is a nine-channel phototube based Cherenkov detector. The gas used is sys-trans-2-butene, held at slightly over atmospheric pressure. The detector consists of aluminum channels 1 cm wide separated by walls which are 250 microns thick. Cherenkov photons are reflected down the polished channels into Hamamatsu R1398 phototubes, which employ a special tube base designed for effective linearity calibration [13].

The counting rates in each detector channel are measured for parallel and anti-parallel combinations of the photon and electron beam helicities. The asymmetry formed from these rates in a given channel i, $A_i{}^m$, is related to the electron polarization measured by the polarimeter ($\mathcal{P}_e^C$) through the following equation

$$A_i{}^m = \frac{N_i^{\rightarrow\leftarrow} - N_i^{\rightarrow\rightarrow}}{N_i^{\rightarrow\leftarrow} + N_i^{\rightarrow\rightarrow}} = \mathcal{P}_e^C \mathcal{P}_\gamma a_i \qquad (6)$$

where $\mathcal{P}_\gamma$ is the circular polarization of the laser beam at the electron-photon crossing point and a_i is the so-called *analyzing power* of channel i. The analyzing power is the convolution of the theoretical Compton asymmetry function with the detector response function for the channel. The response functions are modelled by a detailed EGS Monte Carlo [13]. Including the effects of the response function is a ~1% correction to the theoretical analyzing power (in which the response function is a step function over the width of the channel).

4.2. The Compton Polarized Target

The largest systematic error affecting the polarimeter is the determination of the circular polarization of the target laser, $\mathcal{P}_\gamma$. The problem is that the Compton interaction point is inside the SLC vacuum and analysis optics cannot be placed there. The circular polarization is measured at two other points: on the optics bench after the beam has been polarized, and in an analysis box after the laser exits the vacuum. However, phase shifts induced by the laser transport optics prevent either of these monitors from directly measuring $\mathcal{P}_\gamma$.

The first approach was to measure $\mathcal{P}_\gamma$ intrusively, by breaking the SLC vacuum, and then to use the analysis box optics to measure the stability of the polarization. This technique assumes that the various phase shifts induced by the transport optics remain constant in time, which turned out not to be the case. As a result, for the first 26.9% of the data sample, $\mathcal{P}_\gamma$ was only measured to be (97±2)%.

For the latter 73.1% of the sample, we installed an additional Pockels cell on the source laser bench. The combination of two cells whose principal axes are rotated relatively by 45° allows one to introduce an arbitrary phase shift into the laser beam, which can cancel the transport line phase shifts. By automatically scanning the voltages on the Pockels cell, seeking to maximize the measured Compton asymmetry, the laser polarization was maintained at (99.2±0.6)%.

4.3. Systematic Errors in Polarimetry

Correct measurement of $\mathcal{P}_e^C$ relies on the linearity of the detector and electronics, the determination of the detector location relative to the Compton scattereing spectrum, and the measurement of the target polarization.

The polarimeter linearity is tested by observing the ratio of the experimental asymmetry in a channel with varying phototube gain to that in a channel with constant signal height. This method has the advantage of testing all components of the polarimeter in the same environment in which the data is taken. After sweeping out a linearity curve for a given channel, corrections on the order of 1% are applied to the data. The systematic uncertainty due to detector non-linearity is estimated at 0.6%. Electronic noise and cross-talk have been directly measured, and the effects on measuerd asymmetries are limited to 0.2%.

The energy scale of the polarimeter is calibrated from measurements of the electron kinematic endpoint energy for Compton scattering (17.36 GeV) and the energy at which the asymmetry is zero (25.15 GeV). The position of the kinematic endpoint is determined to within 250 microns by moving the detector platform and observing the falloff in the Compton signal in the outer channels, and comparing the results to a Monte Carlo prediction. Once the absolute detector position is determined in this manner, any relative beam motion is monitored by a ratio of inner channel asymmetries which tracks the location of the zero asymmetry point. The estimated systematic uncertainty for this calibration scheme is 0.4%. We also assume an additional 0.5% uncertainty based on the difference between the measured Compton asymmetry spectrum and the theoretical spectrum (convoluted with the detector response function). This uncertainty is referred to as the *interchannel consistency* because it is measure of the degree to which every detector channel predicts the same electron polarization.

Systematic Uncertainty	$\delta\mathcal{P}_e/\mathcal{P}_e(\%)$
Laser Polarization	1.0
Detector Linearity	0.6
Detector Calibration	0.4
Interchannel Consistency	0.5
Electronic Noise	0.2
TOTAL	1.3

Table 2
Systematic Uncertainties in Polarimetry

The systematic uncertainties that affect the polarization measurement are summarized in Table 2. The laser systematic error is the luminosity-weighted average error of the two laser polarization measurement techniques. The total relative systematic uncertainty is estimated to be $\delta\mathcal{P}_e/\mathcal{P}_e = 1.3\%$.

5. Event Selection

We measure A_{LR} by counting hadronic and $\tau^+\tau^-$ decays of the Z boson for each of the two longitudinal polarization states of the electron beam. The measurement requires knowledge of the absolute beam polarization, but does not require knowledge of the absolute luminosity, detector acceptance, or efficiency.

The Z decays are measured by the SLD detector which has been described elsewhere [14]. The A_{LR} experiment has very little reliance on particle identification or momentum resolution. In order to retain the highest number of events, our analysis is based only on data from the SLD lead-liquid argon sampling calorimeter (LAC) [15].

The triggering of the SLD and the selection of Z events are improved versions of the 1992 procedures. For each event candidate, energy clusters are reconstructed in the LAC. Selected events are required to contain at least 22 GeV of energy observed in the clusters and to manifest a normalized energy imbalance of less than 0.6. The energy imbalance is defined as a normalized vector sum of the energy clusters as follows

$$E_{imb} = \frac{\sum \vec{E}_{cluster}}{\sum |E_{cluster}|}. \quad (7)$$

The left-right asymmetry associated with final state e^+e^- events is diluted by the t-channel photon exchange subprocess. We therefore exclude e^+e^- final states by requiring that each event candidate contain a minimum of 9 clusters (12 clusters if $|\cos\theta|$ is larger than 0.8, where θ is the angle of the thrust axis with respect to the beam axis).

As described in section 3.1, the helicity state of the source electrons is transmitted to the SLD on every beam pulse. The meaning of this transmission, in terms of the beam helicity at the IP (that is, whether the electrons are L or R), is inferred from the sign of the measured Compton scattering asymmetry, the measured helicity of the polarimeter laser, and the theoretical sign of the Compton scattering asymmetry.

A total of 49,392 Z events satisfy the selection criteria. We find that 27,225 (N_L) of the events were produced with the left-handed electron beam and 22,167 (N_R) were produced with the right-handed beam.

We estimate that the combined efficiency of the trigger and selection criteria is (93±1)% for hadronic Z decays. Approximately (0.25±0.1)% of the sample consists of tau pairs. Because muon pair events deposit only small energy in the calorimeter, they are not included in the sample.

The residual background in the sample is due primarily to beam-related backgrounds and to e^+e^- final state events. We use our data and a Monte Carlo simulation to estimate the background fraction due to these sources to be (0.23 ± 0.10)%. The background fraction due to cosmic rays and two-photon processes is (0.02±0.01)%.

6. The Chromaticity Effect

An important issue to address is whether the measured Compton polarization, $\mathcal{P}_e^C$, is equal to the polarization at the SLC interaction point, $\mathcal{P}_e$. As a result of flat beam running, the vertical focusing of the electron beam is limited by third-order chromatic aberrations. That is to say, the focusing of the beam is energy dependent, and thereby the luminosity of the beam is energy dependent. Because the spin precession is also dependent on energy, there will be an energy/polarization correlation, and indeed $\mathcal{P}_e$ will not be equal to $\mathcal{P}_e^C$. This is known as the chromaticity effect. We introduce a paramter ξ, called the *chromaticity correction*, to account for the difference between the two polarizations such that

$$\langle \mathcal{P}_e \rangle = (1+\xi) \langle \mathcal{P}_e^C \rangle . \quad (8)$$

A model based upon the measured energy dependence of the arc spin rotation, $d\theta_s/dE$ = (2.47 ± 0.03) rad/GeV, and the expected dependence of the luminosity on beam energy ($\mathcal{L}(E)$) suggest that ξ is very small ($\xi \leq 0.002$) for the Gaussian core ($\Delta E/E \simeq 0.2\%$) of the beam energy distribution, $N(E)$. However, $N(E)$ is observed to have a low-energy tail extending to $\Delta E/E \simeq 1\%$. This small population of low-energy electrons does not contribute to the luminosity but is measured by the polarimeter, leading to a calculated correction factor, ξ = 0.019 ± 0.005. Measurements of $\mathcal{P}_e$ for different settings of an energy-defining collimator agree well with the predictions of the model.

However, we prefer to employ a conservative and essentially model-independent estimate which implicitly includes the energy tail. The correction ξ is rigorously limited by the following relation:

$$(1+\xi) \leq \left(\frac{\mathcal{P}_e}{\mathcal{P}_e^{linac}}\right)_{max} \cdot \left(\frac{\mathcal{P}_e^{linac}}{\mathcal{P}_e^C}\right)_{max} \quad (9)$$

We determine an upper limit on ξ by finding the upper limits of the two polarization ratios defined in this equation. The first ratio is bounded by a calculation using a purely Gaussian energy distribution of narrow width (0.15% RMS), the measured value of $d\theta_s/dE$, and a chromatically-dominated version of $\mathcal{L}(E)$ to be less than 0.986. The second ratio is bounded by our measurements of spin diffusion in the arc to be less than 1.048. Therefore $1.000 \leq (1+\xi) \leq 1.033$. We use the central value and width of the allowed range, 0 to 0.033, to derive the correction factor, $\xi = 0.017 \pm 0.011$, which is applied to our data.

7. Small Corrections to A_{LR}

The measured asymmetry A_m is related to A_{LR} by the following expression which incorporates a number of small correction terms in lowest-order approximation

$$A_{LR} = \frac{A_m}{\langle \mathcal{P}_e \rangle} + \frac{1}{\langle \mathcal{P}_e \rangle} \Big[f_b (A_m - A_b) - A_{\mathcal{L}} + A_m^2 A_{\mathcal{P}} - E_{cm} \frac{\sigma'(E_{cm})}{\sigma(E_{cm})} A_E - A_\epsilon + \langle \mathcal{P}_e \rangle \mathcal{P}_p \Big] \qquad (10)$$

where f_b is the background fraction; $\sigma(E)$ is the unpolarized Z cross section at energy E; $\sigma'(E)$ is the derivative of the cross section with respect to E; A_b, $A_{\mathcal{L}}$, $A_{\mathcal{P}}$, A_E, and A_ϵ are the left-right asymmetries of the residual background, the integrated luminosity, the beam polarization, the center-of-mass energy, and the product of detector acceptance and efficiency, respectively; and $\mathcal{P}_p$ is any longitudinal positron polarization which is assumed to have constant helicity.

The correction for residual background contamination is moderated by a non-zero left-right background asymmetry ($A_b = 0.031 \pm 0.010$) arising from e^+e^- final states which remain in the sample. The net fractional correction to A_{LR} is $(+0.17 \pm 0.07)\%$.

Residual linear polarization of the polarized electron source laser beam can produce a small left-right asymmetry in the electron current ($\leq 10^{-3}$). The net luminosity asymmetry is estimated from measured asymmetries of the beam current and the rate of radiative Bhabha scattering events observed with a monitor located in the North Final Focus region of the SLC. We determine the left-right luminosity asymmetry to be $A_{\mathcal{L}} = (+3.8 \pm 5.0) \times 10^{-5}$ which leads to a fractional correction of $(-0.037 \pm 0.049)\%$ to A_{LR}. This asymmetry and the left-right asymmetries of all quantities that are correlated with it were reduced by once reversing the spin rotation solenoid at the entrance to the SLC damping ring.

A less precise cross check is performed by examining the sample of 125,375 small-angle Bhabha scattering events detected by the luminosity monitoring system (LUM) [16]. Since the left-right cross section asymmetry for small-angle Bhabha scattering is expected to be very small ($\sim -1.5\times10^{-4}\mathcal{P}_e$ in the LUM acceptance), the left-right asymmetry formed from the luminosity Bhabha events is a direct measure of $A_{\mathcal{L}}$. The measured value of $(-32\pm28)\times10^{-4}$ is consistent with the more precisely determined one.

The polarization asymmetry is directly measured by the polarimter to be $A_{\mathcal{P}} = (-3.3 \pm 0.1) \times 10^{-3}$, resulting in a fractional correction of $(-0.034\pm0.001)\%$ to A_{LR}.

The left-right beam energy asymmetry is directly measured by the energy spectrometer to be $(+4.4\pm0.1)\times10^{-7}$. This effect arises from the small residual left-right beam current asymmetry due to beam-loading of the accelerator and leads to a fractional correction of $(0.00085\pm0.00002)\%$ to A_{LR}.

The value of A_{LR} is unaffected by decay-mode-dependent variations in detector acceptance and efficiency provided that the efficiency for detecting a fermion at some polar angle (with respect to the electron direction) is equal to the efficiency for detecting an antifermion at the same polar angle (which leads to a symmetric acceptance in polar angle). The SLD has a symmetric acceptance in polar angle which implies that the efficiency asymmetry A_ϵ is negligible.

Because the colliding electron and positron bunches are produced on different machine cycles, and because the electron helicity of each cycle is chosen randomly, any positron helicity arising from the polarization of the production electrons is uncorrelated with electron helicity at the IP. The net positron polarization from this process vanishes rigorously. However, positron polarization of constant helicity does affect the measurement. The dominant source of constant-helicity positron polarization is expected to be the Sokolov-Ternov effect in the positron damping ring [17]. Since the polarizing time in the SLC damping rings is about 960 s and the positron storage time is 16.6 ms, the positron polarization emerging from the damping ring is expected to be 1.5×10^{-5}, leading to a maximum fractional correction of 0.011% to A_{LR}.

The corrections listed in equation 10 are found to be small, and are summarized in table 3. These

Correction	$\delta A_{LR}/A_{LR}(\%)$
Background Fraction	0.17 ± 0.07
Luminosity Asymmetry	-0.037 ± 0.049
Polarization Asymmetry	-0.034 ± 0.001
Energy Asymmetry	< 0.001
Efficiency Asymmetry	$\simeq 0$
Positron Polarization	< 0.011
TOTAL	0.10 ± 0.08

Table 3
Summary of small corrections to A_{LR}

corrections change A_{LR} by $(+0.10 \pm 0.08)\%$ of its uncorrected value.

8. Results

The luminosity-weighted average polarization $\langle \mathcal{P}_e \rangle$ is estimated from measurements of $\mathcal{P}_e$ made when Z events were recorded

$$\langle \mathcal{P}_e \rangle = (1+\xi) \cdot \frac{1}{N_Z} \sum_{i=1}^{N_Z} \mathcal{P}_i{}^C = (63.0 \pm 1.1)\% \quad (11)$$

where N_Z is the total number of Z events, and $\mathcal{P}_i{}^C$ is the Compton polarization measurement associated in time with the i^{th} event. The error on $\langle \mathcal{P}_e \rangle$ is dominated by the systematic uncertainties on the polarization measurement and the chromaticity correction, ξ.

The measured left-right cross section asymmetry for Z production is

$$A_m = \frac{(N_L - N_R)}{(N_L + N_R)} = 0.1024 \pm 0.0045. \quad (12)$$

We have verified that A_m does not vary significantly as more restrictive criteria (calorimetric and tracking-based) are applied to the sample and that A_m is uniform when binned by the azimuth and polar angle of the thrust axis.

Using equation 10, we find the left-right asymmetry to be

$$A_{LR}(91.26\,\mathrm{GeV}) = 0.1628 \pm 0.0071(\mathrm{stat.}) \pm 0.0028(\mathrm{syst.}) \quad (13)$$

The various contributions to the systematic error are summarized in Table 4.

Systematic Uncertainty	$\delta A_{LR}/A_{LR}(\%)$
Polarization ($\mathcal{P}_e$)	1.3
Chromaticity (ξ)	1.1
Small Corrections (Eq.10)	0.1
TOTAL	1.7

Table 4
Systematic Uncertainties in A_{LR}

In order to compare with other electroweak measurements, we would like to convert the energy-dependent A_{LR} into a value of $\sin^2\theta_W^{\mathrm{eff}}$. We use a Monte Carlo to correct the result, accounting for photon exchange and for electroweak interference which arises from the deviation of the effective e^+e^- center-of-mass energy from the Z-pole energy (including the effect of initial-state radiation). In units of $\sin^2\theta_W^{\mathrm{eff}}$, the electroweak interference correction is -0.0004. Our calculation agrees with results given by the EXPOSTAR program [18] and by the ZFITTER program [19]. We then find the the effective weak mixing angle and the pole asymmetry A^0_{LR} to be

$$\sin^2\theta_W^{\mathrm{eff}} = 0.2292 \pm 0.0009(\mathrm{stat.}) \pm 0.0004(\mathrm{syst.})$$

$$A^0_{LR} = 0.1656 \pm 0.0071(\mathrm{stat.}) \pm 0.0028(\mathrm{syst.})$$

The quantities A^0_{LR} and $\sin^2\theta_W^{\mathrm{eff}}$ are related by equation 2 and are completely equivalent. We note that this is the most precise single determination of $\sin^2\theta_W^{\mathrm{eff}}$ yet performed.

Combining this value of $\sin^2\theta_W^{\mathrm{eff}}$ with our previous measurement at $E_{CM} = 91.55$ GeV [1], we obtain the value, $\sin^2\theta_W^{\mathrm{eff}} = 0.2294 \pm 0.0010$ which corresponds to the pole asymmetry, $A^0_{LR} = 0.1637 \pm 0.0075$. In either form, this result is smaller by 2.3 standard deviations than the average of 25 measurements performed by the LEP Collaborations [20].

9. Conclusions

The SLD measurement of A_{LR} has become a statistically powerful test of the Standard Model.

This fact is primar:?y due to the increased luminosity of the SLC through flat-beam running, and the increased source polarization through the development of strained-lattice cathodes.

In 1994, we have already measured the polarization from a new strained GaAs cathode to be ~80%. We expect SLC to deliver on the order of 150,000 Zs, thanks to upgrades in the final focus optics. These conditions will improve the error on A_{LR} by a factor of two or better by the end of the 1994 run. If we continue to measure the same central value of $\sin^2\theta_W^{\rm eff}$, the field of electroweak physics will become even more interesting than it already is.

REFERENCES

1. K. Abe *et al.*, *Phys. Rev. Lett.* **70**, 2515 (1993).
2. K. Abe *et al.*, SLAC-PUB-6456, March 1994. Submitted to *Phys. Rev. Lett.*
3. A review of the properties of A_{LR} can be found in D.C. Kennedy *et al.*, *Nuc. Phys.* **B321**, 83 (1989).
4. We follow the convention used by the LEP Collaborations in *Phys. Lett.* **B276**, 247 (1992).
5. N. Phinney, *Int. J. Mod. Phys. A, Proc. Suppl.* **2A**, 45 (1993).
6. C. Adolphsen *et al.*, SLAC-PUB-6118, May 1993.
7. J. Kent *et al.*, SLAC-PUB-4922, March 1989.
8. T. Maruyama *et al.*, *Phys. Rev.* **B46**, 4261 1992.
9. J. Frisch *et al.*, SLAC-PUB-6165, April 1993.
10. T. Limberg, P. Emma, and R. Rossmanith, SLAC-PUB-6210, May 1993.
11. It is important to account for atomic momentum effects in the Møller target. See L.G. Levchuk, KHFTI-92-32, June 1992; and M. Swartz *et al.*, SLAC-PUB-6467, May 1994.
12. M.J. Fero *et al.*, SLAC-PUB-6423, April 1994.
13. R. Elia, Ph.D. Thesis, SLAC Report 429, 1994.
14. The SLD Design Report, SLAC Report 273, 1984.
15. D. Axen *et al.*, *Nucl. Inst. Meth.* **A328**, 472 (1993).
16. S.C. Berridge *et al.*, *IEEE Trans. Nucl. Sci.* **NS-39**, 242 (1992).
17. A.A. Sokolov and I.M. Ternov, *Dokl. Akad. Nauk. SSSR* **153**, 1052 (1963).
18. D.C. Kennedy *et al.*, *Z. Phys.* **C53**, 617 (1992)
19. D. Bardin, *et al.*, CERN-TH. 6443/92, May 1992.
20. The LEP Collaborations: ALEPH, DELPHI, L3, OPAL and the LEP Electroweak Working Group, CERN-PPE/93-157, August 1993.